J. Phycol. **57,** 1212–1222 (2021)

DOI: 10.1111/jpy.13149

PHOTOACCLIMATION STATE OF *THALASSIOSIRA WEISSFLOGII* IS NOT AFFECTED BY CHANGES IN OPTICAL DEPTH UNDER A FLUCTUATING LIGHT REGIME SIMULATING DEEP MIXING[1]

Matthew Brown,[2] *Allen Milligan, and Michael Behrenfeld*

Department of Botany and Plant Pathology, Oregon State University, Corvallis, Oregon 97331, USA

Satellite-based remote sensing allows for global estimates of phytoplankton primary productivity by converting measurements of ocean color or photon absorption into units of carbon fixation. Models which perform this conversion often require an estimate of phytoplankton photoacclimation state such as the carbon to chlorophyll *a* ratio (C:Chl). Recently, our group developed a new photoacclimation model that can be applied to models of primary production. The model assumes that the phytoplankton photoacclimation state is not affected by periods of darkness during deep mixing beneath the photic zone, due to reduction in the plastoquinone pool in darkness and the subsequent deactivation of the signal for chlorophyll synthesis. In this study, we tested these assumptions by culturing the marine diatom *Thalassiosira weissflogii* under fluctuating light conditions simulating three different optical depths with progressively increasing deep mixing periods. The photoacclimation state, measured by the ratio of C:Chl, in *T. weissflogii* was not affected by changes in the length of simulated deep mixing periods. In addition, analysis of photosynthesis vs. irradiance (PE) curves showed that increases in optical depth caused decreases in both the maximum Chl-normalized rate of photosynthesis (P^b_{max}) and in the slope of light-limited photosynthesis (α^b), but had no effect on the half-saturation irradiance (E_k, another metric of photoacclimation). However, measurements of chlorophyll fluorescence during simulated deep mixing did not support the hypothesis that the PQ pool was reduced during dark periods. Thus, our findings support the use of the photoacclimation model for estimating primary production while suggesting the need for further research into the mechanisms controlling photoacclimation in the upper mixed layer environment of the ocean.

Key index words: **E_K independence; fluctuating light; photoacclimation; phytoplankton; *Thalassiosira weissflogii***

***Abbreviations*: C:Chl, carbon to chlorophyll *a* ratio; P^b_{max}, maximum chlorophyll *a*-normalized photosynthesis rate; α^b, chlorophyll *a*-normalized slope of light-limited photosynthesis; E_K, half-saturation irradiance; FRRf, fast repetition rate fluorometry; ST, single turnover; MT, multiple turnover; FmST, single-turnover maximum fluorescence; FmMT, multiple-turnover maximum fluorescence; ST/MT, ratio of single-turnover maximum fluorescence to multiple-turnover maximum fluorescence; PET, photosynthetic electron transport; PQ, plastoquinone**

Phytoplankton in the upper ocean are exposed to a highly variable and rapidly changing light environment. Vertical movement of water can take a phytoplankton cell from full sunlight to complete darkness and back again in the course of a few hours (Denman and Gargett 1983, D'asaro 2003). This presents a dilemma to phytoplankton, as they must absorb enough light to meet their metabolic demands while simultaneously avoiding the damaging effects of excess light, such as the production of reactive oxygen species (Li et al. 2009). Numerous laboratory studies have shown that phytoplankton adjust the content and composition of their photosynthetic machinery in response to changes in irradiance, a process referred to as photoacclimation (Falkowski and Owens 1980, Sukenik et al. 1987, Falkowski and LaRoche 1991, Anning et al. 2000, MacIntyre et al. 2002, Suggett et al. 2007, Vandenhecke et al. 2015).

The basic structure of the photosynthetic electron transport (PET) chain is well described and highly conserved across photosynthetic organisms (Rochaix 2011). The PET chain is comprised of two pigmented light-harvesting photosystems, PSII and PSI, which span the thylakoid membranes within the chloroplast. These photosystems are linked by a series of electron carrying intermediates, including an intramembrane pool of plastoquinone molecules (the PQ pool). Transport of electrons through the PET chain generates a pH gradient across the thylakoid membrane (used to generate ATP), while the electrons themselves are used to generate reductant in the form of ferredoxin and NADPH. In addition to energy and reductant generation, the PET chain also serves as

[1]Received 30 October 2020. Accepted 28 January 2021.
[2]Author for correspondence: e-mail brownma6@oregonstate.edu.
Editorial Responsibility: J. Raven (Associate Editor)

a sensor detecting changes in an organism's light environment (Pfannschmidt and Yang 2012). An increase in light can cause an increase in electron flow through the PET chain beyond the cell's ability to utilize them, resulting in a "backlog" of electrons in the chain. When this happens, most PQ molecules are in a reduced state, whereas in low light, most PQ molecules are in an oxidized state. Sensing such changes in the PQ pool redox state can therefore provide information about the photosynthetic organism's light environment and provides both a signal to the chloroplast and a retrograde signal to the nucleus that may be utilized for photoacclimation. While the full suite of signaling pathways that drive photoacclimation is not yet described, there is evidence that the redox state of the PQ pool is involved.

The redox state of the PQ pool directly influences transcription and translation of genes involved in the production of photosystems, light-harvesting complexes, and enzymes of the chlorophyll synthesis pathway in terrestrial plants (Pfannschmidt et al. 1999, 2001, Frigerio et al. 2007), green algae (Escoubas et al. 1995, Chen et al. 2004), and diatoms (Lepetit et al. 2013). A reduced PQ pool deactivates the signal for chlorophyll synthesis while an oxidized PQ pool activates the signal. Importantly, light is not the only factor influencing the redox state of the PQ pool. In darkness, both eukaryotic and prokaryotic phytoplankton can actively reduce the PQ pool through respiratory processes. In cyanobacteria, reduction in the PQ pool in the dark occurs from respiratory metabolism due to the fact that the respiratory and photosynthetic electron transport chains share the same pool of electron carriers (Mullineaux 2014). In contrast, respiratory control of PQ redox state in eukaryotes requires exchange of reduced carbon metabolites between the mitochondria and chloroplast. Studies have shown that interaction between these organelles is particularly strong in diatoms, due to their close proximity and sharing of outer membranes (Ballieul et al. 2015). Once reductant has been transported to the chloroplast, the PQ pool can be actively reduced in the dark by electron flow through a chloroplast-based NADPH dehydrogenase (NDH) complex (Jans et al. 2008). The NDH complex is part of the chlororespiratory pathway in eukaryotic photosynthetic organisms (Peltier and Cournac 2002). Thus, even in dark environments the degree to which the PQ pool is reduced can serve as a signal regulating chlorophyll synthesis.

A mechanistic understanding of photoacclimation has long been a primary pursuit in photosynthesis research (Baklouti et al. 2006), not only because of its importance to our understanding of cellular processes but also because of its importance at the global level. Satellite ocean color measurements have provided a tool for globally monitoring changes in phytoplankton chlorophyll concentrations and relating these changes to climate variability (Behrenfeld and Falkowsk 1997, Behrenfeld et al. 2005, Westberry et al. 2008, Siegel et al. 2013). The concentration of chlorophyll has also been used to assess ocean net primary production and phytoplankton biomass (Behrenfeld and Falkowsk 1997). The concentration of chlorophyll *a* on its own, however, cannot be taken as a proxy for phytoplankton biomass since changes in chlorophyll *a* may indicate either changes in the standing stock of phytoplankton or changes in cellular chlorophyll content due to photoacclimation.

In recent years, models have been developed which calculate NPP based either on phytoplankton absorption coefficients (Lee et al. 1996, Smyth et al. 2005) or on estimates of phytoplankton carbon (Behrenfeld et al. 2005, Westberry et al. 2008). Absorption-based models derive NPP from the product of absorbed light (Q_{par}) and the efficiency of the conversion of photons into biomass ($\phi\mu$), while carbon-based models calculate NPP as the product of phytoplankton growth rate (μ) and the concentration of phytoplankton carbon (C_{phyto}). The recently developed CAFE model combines these approaches to allow for a mechanistic determination of phytoplankton growth rate which, combined with estimates of C_{phyto}, allows a more accurate estimate of NPP (Silsbe et al. 2016). While the CAFE model provides a number of advantages over previous approaches, it still must take into account changes in cellular physiology and growth driven by photoacclimation. In most NPP models, the estimate of photoacclimation state is either the carbon:chlorophyll ratio (θ or C:Chl) or a parameterization of the saturation irradiance for photosynthesis (E_k; e.g., Westberry et al. 2008). In a previous paper (Behrenfeld et al. 2015), we developed an algorithm for deriving estimates of C:Chl from satellite measurements of ocean color. This algorithm has been used to provide an estimate of E_k in the CAFE model (in which E_k is correlated with C:Chl; Silsbe et al. 2016).

With respect to satellite data, it is the photoacclimation state of cells within the active mixing layer that is of primary concern because the signal detected by satellite ocean color sensors emanates from very near the surface (i.e., primarily within the mixing layer). Accordingly, an understanding of how phytoplankton acclimate to the highly fluctuating light environment of the mixed layer is imperative. Previous approaches have described the photoacclimation state as a function of the median light level within the mixed layer (Behrenfeld et al. 2005, Westberry et al. 2008). In environments where the mixed layer is deeper than the photic zone, this results in a very low median light level, as the dark periods experienced by the cell during deep mixing are included in the calculation. In

our revised algorithm (Behrenfeld et al. 2015), we describe photoacclimation in a deeply mixing water column as a function of the median light level within the photic zone alone, rather than the whole mixed layer. This revision was made by assuming that the PQ pool will be reduced in the dark depths of the mixed layer as a result of chlororespiration (Peltier and Cournac 2002) and that this reduced PQ pool should deactivate the signal for photoacclimation.

One method for estimating PQ pool redox state is through measurements of chlorophyll fluorescence. The basis of this technique (Kolber et al. 1998) is that the energy of an absorbed photon has several possible fates. Primarily, it can be used in photochemistry, converted to heat via non-photochemical quenching (NPQ), or rereleased as a photon (i.e., fluorescence; Baker 2008). As these pathways are in competition, applying a saturating flash of light and measuring the amount of fluorescence over time can provide information about the kinetics of electron transfer in the PET chain. The shape of the fluorescence transient (i.e., the curve produced by measurement of fluorescence under a saturating flash of light) is affected by changes in PQ pool redox state. Reducing the pool or decreasing the rate at which the pool is oxidized causes fluorescence to rise rapidly at the onset of a flash sequence (Toth et al. 2007, Prasil et al. 2018).

In this study, we tested assumptions of our photoacclimation algorithm in a laboratory setting using the marine diatom *Thalassiosira weissflogii* grown under simulated natural light conditions of the upper ocean mixing layer. We examined how the photoacclimation state changes in response to increasing periods of darkness during the daytime (simulating mixing to depths greater than the photic layer). We measured changes in cellular pigment content and chemical composition to determine C:Chl under each light regime. In addition, we measured photosynthetic carbon fixation as a function of instantaneous irradiance (i.e., photosynthesis vs. irradiance curves) to determine whether photosynthetic parameters (including E_k) were affected by our simulated mixing layer light regime. Finally, we tested our hypothesis regarding the effect of PQ pool redox state on photoacclimation during deep mixing using chlorophyll fluorescence measurements.

METHODS

Growth conditions. Cultures of *Thalassiosira weissflogii* were grown in f/2 media under several fluctuating light regimes simulating the light environment of the upper mixed layer of the ocean (D'asaro 2003). Cultures were diluted every 2-3 d and acclimated for 7-10 generations before sampling. This dilution period was chosen to maintain cells in exponential growth phase and to prevent self-shading. Cell counts within culture varied between $2*10^4$ and $1*10^5$, and cultures remained visually transparent even at the highest cell count. Light was provided by a custom LED Phyto-panel (Photon Systems Instruments) comprised of white light LED's. All cultures were grown on a 12:12-h light:dark cycle. Irradiance varied during the day period from total darkness up to 1600-1800 μmols photons $\cdot$ m^{-2} $\cdot$ s^{-1}. The different fluctuating light regimes simulated different mixed layer depths, specifically simulating mixing to 5, 10, and 15 optical depths (hereafter OptD5, OptD10, OptD15, respectively). Optical depth is related to the absorbance of the medium (i.e., Beer-Lambert law) and is defined as $OptD = k_d z$, where k_d is the diffuse attenuation coefficient and z is the physical depth.

Irradiance was measured continuously using a 4π light sensor (Licor). The sensor was immersed in water and placed at a similar distance from the light bank as the samples. Median irradiance for the mixed layer (Table 1) was calculated as the median of all values measured during the 12-h photoperiod. Median irradiance for the euphotic zone (Table 1) was calculated as the median of all values measured when irradiance exceeded 0.5 μmols photons $\cdot$ m^{-2} $\cdot$ s^{-1}. Unless otherwise stated, for all analyses described below the samples were collected from the cultures pre-dawn immediately before the onset of light to avoid potentially confounding issues of changes in cellular properties that can occur over the photoperiod.

Chlorophyll, carbon, and nitrogen. For assessments of chlorophyll *a* concentration, between 8 and 12 mL of culture sample were filtered on Whatman 25 mm GF/F filters (Whatman, Little Chalfont, UK) and placed in sealed tubes containing 5 mL of 90% acetone. Filters were kept in darkness overnight at 8°C. Filters were then removed, and the tubes were centrifuged to clarify extracted pigments. Absorption of chlorophyll extract was measured in a Shimadzu UV-2401 PC dual-beam spectrophotometer, and chlorophyll *a* concentrations were determined following the equations of Ritchie (2006) for diatoms.

To determine cellular content of carbon and nitrogen, pre-dawn samples were taken from each culture. Cell concentration for each sample was measured using a Beckman Multisizer 3 Coulter Counter, followed by the division of the sample into three replicates of different volumes: a 3 mL replicate, a 4 mL replicate, and a 5 mL replicate for determination of carbon and nitrogen content. Each replicate was then filtered onto pre-combusted 25mm Whatman GF/F filter, immediately frozen at −80°C, and stored until the time of measurement. Prior to measurements, replicates were

TABLE 1. Growth rate and irradiance. Median mixed layer irradiance was calculated by taking the median value of all light measurements during the day period. Median euphotic irradiance was calculated by only taking the median value of light measurements during the day period above 0.5 μmol photons $\cdot$ m^{-2} $\cdot$ s^{-1}. Total daily irradiance is the sum of all daily light measurements. Standard deviation is in parentheses.

Optical Depth	μ(d^{-1})	Median Mix Layer Irr (μmol photons $\cdot$ m^{-2} $\cdot$ s^{-1})	Median Euphotic Irr (μmol photons $\cdot$ m^{-2} $\cdot$ s^{-1})	Total Daily Irradiance (μmol photons $\cdot$ m^{-2} $\cdot$ s^{-1})
5	0.74 (0.05)	48.61 (3.58)	199 (9.5)	$8.921*10^6$ ($4.35*10^5$)
10	0.40 (0.06)	0.0	259 (19)	$5.163*10^6$ ($4.06*10^5$)
15	0.42 (0.03)	0.0	276 (11)	$4.350*10^6$ ($1.98*10^5$)

dried overnight in an oven at 50°C. Chemical composition was then determined with an Exeter Analytical Ce-440 Elemental Analyzer that was calibrated using acetanilide standards. Each set of three replicates was then fitted with a linear regression, from which the amount of carbon and nitrogen present in 1 mL of sample was determined. To correct for extracellular carbon present in the sample media, the y-intercept value was subtracted from all measured values. Finally, the calculated carbon and nitrogen concentration were then normalized to the measured cell concentration (mL^{-1}) of their respective sample.

Photosynthesis-irradiance curves. For our OptD5 and OptD15 treatments, pre-dawn samples were collected to determine photosynthetic carbon uptake rates as a function of instantaneous irradiance using the photosynthetron method of Lewis and Smith (1983). A sample of each culture was taken, inoculated with 50 µL of the radioactive tracer $NaH^{14}CO_3$, and split between 13–15 scintillation vials. Specific activity was determined by fixing a 950 µL sample with phenethylamine. Each vial contained exactly 1 mL of sample. Vials were placed in a photosynthetron (CHPT Mfg Inc; Georgetown, DE) where each was exposed to a single irradiance level between 0 and 1200 µmols photons · m^{-2} · s^{-1} for 20 min. Subsequently, vials were removed and 50 µL of 10% HCl was added to each to convert any remaining $NaH^{14}CO_3$ to $^{14}CO_2$ and degassed overnight. Activity in each vial was determined using a scintillation counter (Beckman LS6500) and applying the instrument quench correction. Total carbon uptake per sample was normalized to chlorophyll *a* of the sample, and results were fitted using a hyperbolic tangent function (Jassby and Platt 1976). From this fit, we calculated several photosynthetic parameters: the chlorophyll *a*-normalized maximum photosynthetic rate (P^b_{max}); the chlorophyll *a*-normalized slope of light-limited photosynthesis (α^b); and the saturation irradiance ($E_k = P^b_{max}/\alpha^b$).

Chlorophyll fluorescence. Variable fluorescence measurements were made on samples from each mixing layer light regime following methods similar to those used in Brown et al. (2019). A culture sample (~1.5 mL) was placed into a glass cuvette within a Soliense LIFT-FRR. Since diatom NPQ does not relax in the dark, samples were low-light acclimated at 10-20 µmols photons · m^{-2} · s^{-1} (Milligan et al. 2012). Measurements used a blue-light diode with an emission wavelength of 475 nm. The FRR excitation protocol had four distinct phases (see Kolber et al. 1998; Fig. S1 in the Supporting Information). The first phase entailed a saturation sequence of flashlets applied in ~ 200 µs (termed the single-turnover phase; ST). Each individual flashlet lasted 0.7 µs and was separated by a gap of 1.5 µs, for a total of 100 flashlets. The second phase was a relaxation sequence of 127 flashlets beginning with a gap of 20 µs that increased exponentially toward the end of the sequence (dark multiplier 1.1). The third phase entailed a sequence of 3500 flashlets lasting 2 µs each and with a 40-µs gap. This phase (the multiple-turnover phase; MT) lasted for a total of ~ 150 ms. The final phase of the protocol was a second relaxation sequence with identical parameters as the first relaxation sequence.

Two different sampling procedures were used in this study for FRRf fluorescence measurements. In the first, fluorescence measurements were taken immediately before the onset of light at dawn. This was to determine the maximum photosynthetic efficiency and to determine the shape of the fluorescence transient in the absence of NPQ. Samples were taken directly from the culture vessel, low-light acclimated for at least 10 minutes, and placed into a FRRf cuvette for a 10-min dark acclimation prior to measurement. Our second measuring procedure was used to determine if the PQ pool was reduced during simulated deep mixing periods. Multiple fluorescence measurements were taken during two distinct periods of simulated light regime during our OptD15 mixing depth treatment (Fig. 1B). First, measurements were taken toward the end of a light period just before cultures entered a dark period. Light levels during this "transition period" were between 10–60 µmol photons · m^{-2} · s^{-1}. Second, measurements were taken during dark periods that simulated deep mixing below the photic zone. These "dark" period measurements were taken at roughly the halfway point of the deep mixing regime, roughly 30 min after the onset of darkness (Fig. 1B). To ensure that the redox state of the PQ pool was not altered, the entire measurement was performed in darkness. The FRRf was placed next to the culture vessels and covered with black cloth. A piece of thin plastic tubing was connected from the FRRf cuvette to the culture vessels, such that the tube remained completely under the black

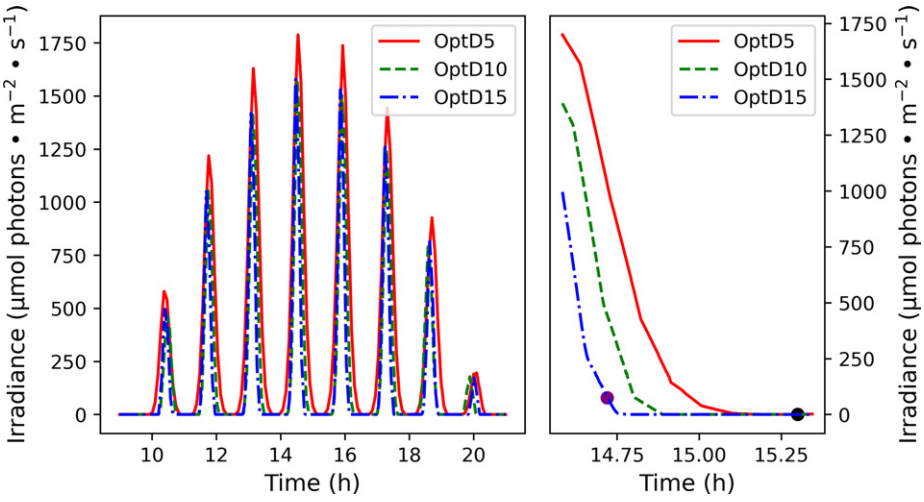

FIG. 1. (A) Daily irradiance profile for our three light regimes (OptD5, OptD10, OptD15). (B) View of Graph A between 14.6 h and 15.4 h. The red dot represents the time at which the "transition" fluorescence measurements were taken, and the black dot represents the time the "dark" measurements were taken. Time on both graphs refers to the hour of the day on a 24-h clock.

cloth. Using a computer-controlled peristaltic pump, a 2 mL volume of sample was pulled directly from the culture vessel into the cuvette and a fluorescence measurement was taken.

Statistics. To detect statistical differences between our different simulated mixing regimes, we performed analysis of variance (ANOVA) tests on our data. P-values below 0.05 were considered to be statistically significant. All statistical analyses were performed using the scipy module in Python.

RESULTS

Phytoplankton growth rates for the three simulated mixing regimes were 0.74 · d^{-1}, 0.40 · d^{-1}, and 0.42 · d^{-1} for cells growing in the OptD5, OptD10, and OptD15 simulated mixed layers, respectively (Table 1). The growth rate for cells in the OptD5 mixed layer was significantly higher than that of cells in OptD10 and OptD15 mixed layers. Growth rates of cells did not significantly differ between the OptD10 and OptD15 mixed layer.

Cellular composition. Cellular chlorophyll *a* content was 2.93, 2.96 and 3.13 pg Chl *a* · $cell^{-1}$ for OptD5, Opt10, and OptD15, respectively (Fig. 2). No significant differences were observed in content of chlorophyll *a* per cell between our three optical depths. Cellular carbon content was 62, 63, and 75 pg · $cell^{-1}$ for OptD5, OptD10, and OptD15, respectively, and did not significantly differ from each other (Fig. 3). Conversely, cellular nitrogen content in our three treatments was significantly lower in our OptD5 and OptD10 treatments (16 and 17 pg · $cell^{-1}$, respectively) compared with our OptD15 treatment (24 pg · $cell^{-1}$; Fig. 3). Finally, the ratio of cellular carbon to chlorophyll *a* (C:Chl) for our three optical depths was 21.1, 24.8, and 22.8, respectively, and did not significantly differ between treatments (Fig. 4).

Photosynthesis-irradiance curves. Comparison of carbon uptake between our OptD5 and OptD15 treatments revealed significant differences in photosynthetic parameters (Fig. 5). The maximum

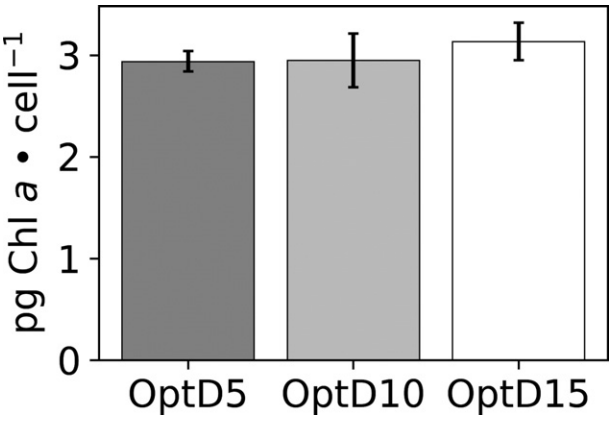

FIG. 2. Cellular chlorophyll *a* content in pg · $cell^{-1}$. Each value is the average of nine independent replicates (three technical, three biological) for each light treatment. Error bars represent 1 standard deviation.

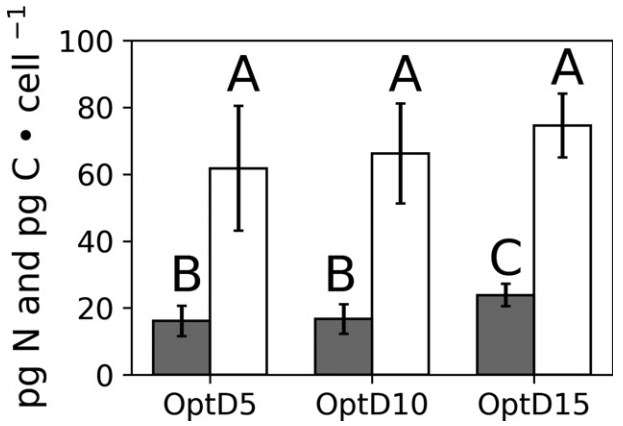

FIG. 3. Cellular nitrogen content (gray) and cellular carbon content (white) in pg · $cell^{-1}$. Error bars represent one standard deviation. Different letters represent treatments which differed by $p < 0.05$.

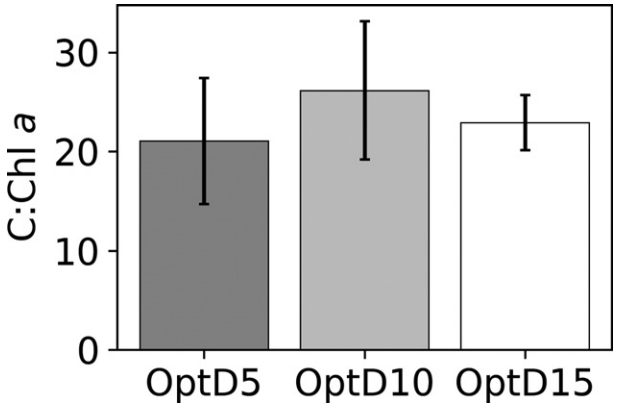

FIG. 4. Ratio of cellular carbon to chlorophyll *a* concentration. Error bars represent 1 standard deviation.

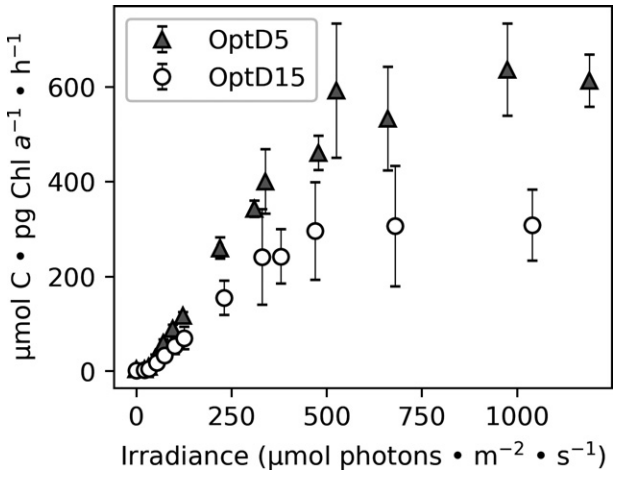

FIG. 5. Photosynthesis vs. irradiance curves taken from OptD5 (triangles) and OptD15 (circles) cultures. Error bars represent 95% confidence intervals, derived from three independent replicates.

rate of Chl *a*-normalized carbon uptake (P^b_{max}) from the OptD5 treatment was 652 μmol C · pg Chl a^{-1} · h^{-1} and significantly higher (p = 0.01) than the value of 334 μmol C · pg Chl a^{-1} · h^{-1} found for the OptD15 treatment (Table 2). Cells from the OptD5 treatment also showed a significantly higher (p = 0.049) initial light-limited slope (α^b) of the photosynthesis-irradiance curve (1.27 μmol C · pg Chl a^{-1} · h^{-1}/μmol photons · m^{-2} · s^{-1}) compared with the OptD15 treatment (0.77 μmol C · pg Chl a^{-1} · h^{-1}/μmol photons · m^{-2} · s^{-1}). Finally, the saturation irradiance (E_k) did not significantly differ (p = 0.47) between cells from the OptD5 (512 μmol photons · m^{-2} · s^{-1}) and OptD15 (434 μmol photons · m^{-2} · s^{-1}) treatments.

Fluorescence. Pre-dawn fluorescence measurements did not differ between the OptD10 and OptD15 treatments (Fig. 6). In contrast, fluorescence measurements from the OptD5 treatment showed a slower rise in the initial portion of the MT phase (up to 1000 flashlets) and achieved a lower level of maximum fluorescence at the end of the MT phase in comparison with our other treatments.

Comparison of fluorescence measurements taken after the onset of the light period showed significant differences. Fluorescence measurements taken during the transition period showed a faster rise in fluorescence during the initial portion of the MT phase in comparison with measurements taken during the dark periods (Fig. 7). This suggests a more reduced PQ pool during the transition period. Maximum fluorescence achieved at the end of the MT phase did not differ significantly.

DISCUSSION

Photoacclimation. Over the last half-century, a great deal of research has been performed on how phytoplankton acclimate to changes in their light environment (e.g., Falkowski and Owens 1980, Sukenik et al. 1987, Falkowski and LaRoche 1991, Anning et al. 2000, MacIntyre et al. 2002, Suggett et al. 2007, Vandenhecke et al. 2015). The majority of this research has examined the effects of changes in static light intensity (as opposed to dynamic light regimes) and, as a rule, show that phytoplankton cellular chlorophyll *a* content exhibits a negative exponential relationship with growth irradiance.

Generally, studies employing fluctuating light regimes have compared the observed photoacclimation response to that found under static or

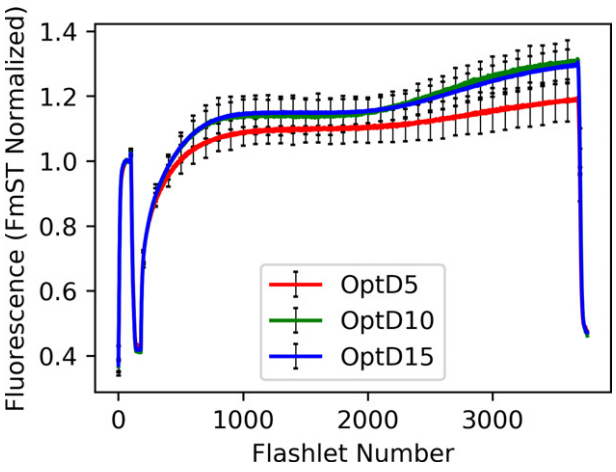

FIG. 6. Dark acclimated fast repetition rate fluorometry (FRRf) curves. Each curve is the average of measurements taken over 5-7 d. Error bars represent 1 standard deviation.

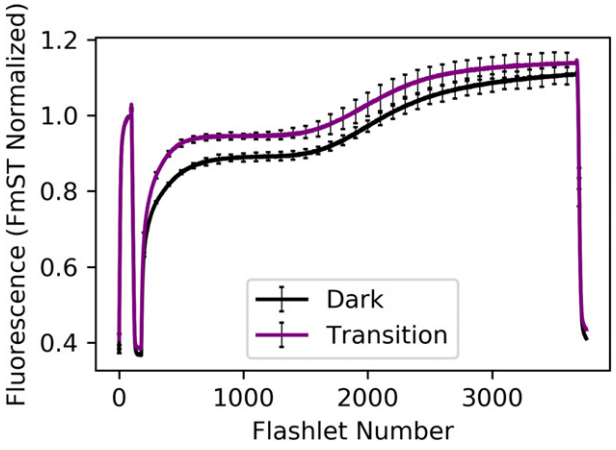

FIG. 7. FRRf transients taken during the day period of the OD30 simulated mixing regime. Measurements were taken during periods of simulated deep mixing beneath the photic zone (dark) and during periods of low light (10-60 μmol photons · m^{-2} · s^{-1}) immediately prior to the "dark" periods (transition). Each transient is the average of three independent biological replicates, and error bars represent 1 standard deviation.

TABLE 2. Photosynthetic parameters as determined from 20-minute carbon uptake measurements. PI curves for each treatment were averaged and parameters were calculated by fitting ^{14}C data to a hyperbolic tangent function. Numbers in parentheses represent one standard deviation. A * indicates a p-value less than 0.05. P^b_{max} – chlorophyll *a*-normalized maximum rate of carbon uptake. α^b – chlorophyll *a*-normalized slope of light-limited photosynthesis. E_k – saturation irradiance (P^b_{max}/α^b).

Optical depth	P^b_{max} (μmol C · mg Chl *a* · h^{-1})	α^b (μmol C · m^{-2} · s^{-1} · mg Chl a^{-1} · h^{-1} · μmol photons^{-1})	E_k (μmol photons · m^{-2} · s^{-1})	Daily Integrated Carbon fixation (g fixed C · g cellular C^{-1} · d^{-1})
5	652 (66)*	1.27 (0.10)*	512 (66)	1.37
15	334 (86)*	0.77 (0.23)*	434 (172)	0.38

sinusoidal light conditions of similar mean light intensity (e.g., Fietz and Nicklisch 2002, van de Poll et al. 2007). A few studies have compared the effects of different fluctuating light regimes (Havelkova et al. 2004, Shatwell et al. 2012), and a small number have examined photoacclimation under simulated "deep mixing" (Ibelings et al. 1994, Milligan et al. 2012). In contrast to the near-universal response of phytoplankton to increases in light intensity under static light, responses to fluctuating light conditions appear to be highly species specific. In Mills et al. (2010), moving from a deep-mixing regime (mean light intensity 65 μmol photons · m^{-2} · s^{-1}) to a shallow mixing regime (mean light intensity 250 μmol photons · m^{-2} · s^{-1}) caused a decrease in chlorophyll *a* per cell in two species but had no effect in the third. In Fietz and Nicklisch (2002), shifting from a sinusoidal light regime to a fluctuating light regime of equivalent light intensity caused a small but non-significant decrease in chlorophyll *a* in one species and a significant increase in another. For some species, it appears that the maximum irradiance as well as the average irradiance contributes to the photoacclimation response (van de Poll et al. 2007).

To our knowledge, no previous study has examined the response of phytoplankton to different periods of darkness under a light regime which simulates the natural light conditions of the upper ocean. Previous research on the effect of photoperiod length on photoacclimation suggests that in many cases it is light intensity, not photoperiod, that controls pigment production (Verity 1981, Tang and Vincent 2000). Changes in light intensity alter the rate at which electrons from PSII are delivered into the PQ pool. In the absence of a simultaneous change in the PQ pool's oxidation rate, the redox state of the pool will consequently change, thus altering gene expression and triggering a photoacclimation response (Escoubas et al. 1995). Conversely, changes in the length of the photoperiod are not expected to alter the PQ pool's redox state and thus should have no effect on photoacclimation state. The Behrenfeld et al. (2015) photoacclimation model does not take daylength into account when deriving estimates of C:Chl and, under deep mixing conditions, assumes that C:Chl is insensitive to time spent in darkness beneath the photic zone. The model yields C:Chl values that are highly correlated with those measured from satellites.

Results of the current study indicate that changes in deep mixing depth where median irradiance is held constant have no effect on the cellular C:Chl ratio. However, our findings are not consistent with the assumption of the Behrenfeld et al. (2015) model that this insensitivity to periods of darkness is due to PQ pool redox regulation of photoacclimation. Specifically, our fluorescence measurements taken during the dark periods show a slower rise in fluorescence compared with measurements taken under low light (Fig. 7), suggesting that the PQ pool was less reduced in the dark (Toth et al. 2007). It should be noted that the rise in fluorescence is affected not just by the redox state of the PQ pool but also by the relative PQ pool reduction and oxidation rates (Brown et al. 2019). Analysis of the single-turnover decay phase of our fluorescence data allows for the calculation of the minimum turnover time (τ) of various stages of electron transport. The decay is generally assumed to be a three-phase exponential decay (see Kolber et al. 1998), although in the case of our data, the third τ component is poorly fit and thus not reported. These values provide a measurement of how quickly electrons are moving through the PET chain and thus to the relative PQ pool reduction and oxidation rates. Minimum turnover times were slightly, though significantly (p-value < 0.05), lower in our transition measurements than our dark measurements (Table 3), meaning that fluorescence rose at a faster rate in the transition measurement despite a faster rate of electron transport. We conclude that differences in the PQ pool redox state (i.e., a less reduced pool during deep mixing) are the best explanation for our data. Thus, our findings suggest that the PQ pool redox state during deep mixing is not the central regulating mechanism making photoacclimation state insensitive to periods of darkness. Assuming this conclusion is correct, we propose an alternative explanation for this insensitivity of photoacclimation to darkness in *Thalassiosira weissflogii*.

Photoacclimation. While PQ pool redox state is a major regulator of photoacclimation, the process of chlorophyll and light-harvesting antenna protein production is controlled at multiple levels of cellular regulation. Beginning with the precursor molecule δ-aminolevulenic acid, chlorophyll synthesis proceeds through a 17-step biochemical pathway (Bollivar 2006). The penultimate step in this pathway is the conversion of protochlorophyllide (Pchlide) to chlorophyllide by the enzyme protochlorophyllide oxidoreductase. This step appears to be one of the most important steps regulating chlorophyll synthesis (Reinbothe et al. 2010). Two distinct enzymes are known to catalyze this reaction:

TABLE 3. Minimum turnover time of electron transport. Values were calculated from the single-turnover decay phase of fluorescence transients taken during either the low-light transition period of the light regime or the dark period during simulated deep mixing. Numbers in parentheses are one standard deviation. A * indicates a p-value less than 0.05.

	τ_1 (μs)	τ_2 (μs)
Transition	699 (38)*	7354 (234)*
Dark	773 (37)*	8824 (318)*

a light-dependent version (POR) and a light-independent version (LIPOR).

The first enzyme, POR, is present in virtually all species of cyanobacteria, eukaryotic algae, and land plants (Hunsperger et al. 2015). Its reaction requires the absorption of a photon by its substrate Pchlide in addition to the use of reductant derived from light absorption like NADPH (Reinbothe et al. 2010). The second enzyme, LIPOR, is evolutionarily closely related to the nitrogenase enzyme and able to operate in the absence of light. The three genes which code for LIPOR have been lost in a number of algal groups, including members of the Rhodophyta, Haptophyta, and Stramenopila (like diatoms). While the genome of *Thalassiosira weissflogii* has not been sequenced, analysis of the genomes of six widely divergent diatom species (*Phaeodactylum tricornutum*, *Fisulifera* sp., *Odeontella sinesis*, *Synedra* sp., *Thallasiosira pseudonana*, *Thallasiosira oceanica*) found no copies of or genes homologous to the LIPOR gene (Hunsperger et al. 2015), suggesting that the genes are uncommon if not absent from the diatom lineage. The inability to convert Pchlide to Childe in the dark would cause an increase in the concentration of the former. The rate of synthesis of δ-aminolevulenic acid is known to be inversely proportional to the concentration of Pchlide (Richter et al. 2010), and there is evidence that Pchlide acts as a negative feedback control on δ-aminolevulenic acid production in conjunction with other chlorophyll synthesis enzymes (Kauss et al. 2012). As species lacking LIPOR are incapable of synthesizing chlorophyll in the dark, we propose that the lack of change in C:Chla in *T. weissflogii* across fluctuating light regimes in this experiment was not due to downregulation of chlorophyll synthesis in response to a reduced PQ pool (as envisioned by Behrenfeld et al. 2015) but rather reflects the inactivation of POR in the dark coupled with the absence of LIPOR and the negative feedback effect of PChlide.

While the above proposal explains why deep mixing has no effect on photoacclimation state in *Thalassiosira weissflogii*, other mechanisms may achieve the same result in different species. For example, numerous phytoplankton species possess LIPOR, including members of the widespread cyanobacterial genera *Prochlorococcus* and *Synechococcus* (Fong and Archibald 2008). In cyanobacteria, however, the PQ pool is shared between photosynthesis and respiration, and based on field fluorescence measurements is known to be reduced in the dark (Behrenfeld and Kolber 1999, Behrenfeld and Milligan 2013). In these cases, photoacclimation state may also be insensitive to deep mixing (i.e., deeper that the photic layer) because reduction in the PQ pool due to dark respiration deactivates chlorophyll synthesis. Thus, multiple approaches may have evolved in different algal lines to sequester photoacclimation processes in the dark, but irrespective of approach they would all be consistent with the fundamental concept introduced in the Behrenfeld et al. (2015) photoacclimation model.

Photosynthetic parameters. The shape and parameters of a photosynthesis versus irradiance (PE) curve reflect the balance between the absorption of light energy and its conversion into chemical energy, and utilization of this chemical energy in metabolic processes. At low irradiance, photosynthesis increases linearly with light, as light absorption is the factor limiting photosynthesis. When normalized to chlorophyll *a*, this initial light-limited slope is denoted α^b. At higher irradiances, light absorption can vastly exceed the capacity of the cell to utilize absorbed energy and carbon fixation reaches an asymptote. This maximum rate of photosynthesis, normalized to chlorophyll *a*, is denoted P^b_{max}. Taking the ratio between these two parameters (P^b_{max}/α^b) provides an index of the irradiance level at which electron transport through the PET chain is roughly in balance with energy utilization for carbon fixation. Changes in this saturation irradiance (denoted E_k) are commonly associated with photoacclimation (Behrenfeld et al. 2004).

P^b_{max} and α^b were 50% and 40% lower in our OptD15 culture than in our OptD5 culture, respectively, but E_k did not significantly differ between treatments (Table 2). Thus, our cultures appeared to acclimate to changes in simulated mixing in an "E_k-independent" manner. This phenomenon was first reviewed in Behrenfeld et al. (2008), where it was hypothesized that correlated changes in P^b_{max} and α^b were due to direct use of photosynthetically derived carbon in mitochondrial respiration (i.e., substrate shuttling). Subsequent research showed that E_k-independent photoacclimation was largely attributable to physiological changes in how cells utilize photosynthetically derived carbon (Halsey et al. 2010, 2013, 2014, Fisher and Halsey 2016). In slow-growing cells, either nutrient- or light-limited, a large proportion of photosynthate is directed into a pool of short-lived (<20 min) carbon molecules that are rapidly utilized in respiration (thus consuming O_2). As growth rate increases, cells increasingly devote photosynthate to produce reductants that can be used for longer-lived (>20 min) and more reduced carbon products, such as membrane lipids (Halsey et al. 2010, 2013, 2014, Fisher and Halsey 2016). While the transient carbon products used for either fate are ultimately not retained as cellular carbon biomass (i.e., do not contribute to NPP), the different lifetimes of the pools and the changes in carbon partitioning between them across growth rates result in the observed E_k-independent changes in P^b_{max} and α^b. Based on the current results, we suggest that similar changes in the partitioning of photosynthetically derived carbon are responsible for the E_k-independent behavior observed between mixing regimes in the current study. Specifically, cells in the faster growing OptD5 treatment would

be expected to direct a greater proportion of fixed carbon to longer-lived transient carbon pools, while cells from the slower growing OptD15 treatment would primarily utilize fixed carbon in respiration.

If our interpretation is correct, then it could solve an apparent contradiction between our PE data and the predictions of the Behrenfeld photoacclimation model. In the model, Pmax is assumed to be a constant while P^b_{max} is proportional to the cellular C: Chl (Behrenfeld et al. 2015). Our data would seem to be in contradiction to this, as we observed large changes in P^b_{max} without concurrent changes in C: Chl. However, the photoacclimation model assumes that P^b_{max} is measuring net primary production (NPP). As previous studies of E_k independence have shown (Halsey et al. 2010, 2013, 2014, Fisher and Halsey 2016), whether or not carbon fixation measurements provide estimates of NPP is dependent on the time period of the measurement (e.g., 20-min versus 24 h) and the growth rate of the cells being sampled. At slower growth rate, a 20-min carbon fixation measurement provides an estimate of NPP. As growth rate increases, the measured amount of carbon fixed increasingly provides an estimate of gross primary production (GPP; Halsey et al. 2010, 2013). Further support for this comes from comparing the daily integrated carbon fixation rates (g fixed C · g cellular C · d^{-1}) for our two optical depths with their measured growth rates. Phytoplankton growth rate calculated from our measured ^{14}C uptake data and integrated over the photoperiod for our OptD15 treatment was 0.38 · d^{-1}, which is very close to the directly measured growth rate of 0.42 · d^{-1}. In contrast, growth rate calculated from our measured ^{14}C uptake data for the OptD5 treatment was 1.37 · d^{-1}, which is significantly higher than the directly measured growth rate of 0.72 · d^{-1} (Table 2). These findings provide additional support for our interpretation of the E_K-independent differences in ^{14}C uptake data observed between treatments and are consistent with expectations of the Behrenfeld photoacclimation model.

CONCLUSIONS

Remote sensing is a tremendously useful tool that allows global assessments of phytoplankton physiology and production. However, accurate estimates of phytoplankton primary production require an accurate understanding of how phytoplankton photoacclimate to the conditions they experience in the upper mixed layer. Results of this study show that the photoacclimation state of the marine diatom *Thalassiosira weissflogii* is not affected by simulated deep mixing below the photic zone, thus confirming the main conclusion of the Behrenfeld photoacclimation model (2015). In addition, we have shown that *T. weissflogii* acclimated to changes in the depth of the mixed layer in an E_k-independent manner. Both findings have important implications for the construction of models of satellite-derived primary production. Our results suggest that PQ pool redox sensing is not the primary regulatory mechanism responsible for the insensitivity of photoacclimation to periods of dark exposure in *T. weissflogii*, and we instead propose an alternative regulatory mechanism beginning with the final step in chlorophyll synthesis. We note, however, that other regulatory pathways may be employed by other marine species to achieve the same end. Retrograde signaling from the chloroplast to the nucleus, necessary for photoacclimation, is known to proceed through a number of different mechanisms (Escoubas et al. 1995, Strand et al. 2003, Moller and Sweetlove 2010). Future studies are needed to further examine the diversity of these pathways among ocean phytoplankton to better inform the construction of improved photoacclimation models.

This study was funded in part by a NASA Earth and Space Science Fellowship.

CONFLICT OF INTEREST

The authors list no conflicts of interest.

Anning, T., MacIntyre, H., Pratt, S., Sammes, P., Gibb, S. & Geider, R. 2000. Photoacclimation in the marine diatom *Skeletonema costatum*. *Limnol. Oceanogr.* 45:1807–17.

Baker, N. 2008. Chlorophyll fluorescence: a probe of photosynthesis *in vivo*. *Annu. Rev. Plant Bio.* 59:89–113.

Baklouti, M., Diaz, F., Pinazo, C., Faure, V. & Queguiner, B. 2006. Investigation of mechanistic formulations depicting phytoplankton dynamics for models of marine pelagic ecosystems and description of a new model. *Prog. Oceanogr.* 71:1–33.

Ballieul, B., Berne, N., Murik, O., Petroutsos, D., Prihoda, J., Tanaka, A., Villanova, V. et al. 2015. Energetic coupling between plastids and mitochondria drives CO_2 assimilation in diatoms. *Nature* 524:366–69.

Behrenfeld, M. & Falkowski, P. 1997. A consumer's guide to phytoplankton primary productivity models. *Limnol. Oceanogr.* 42:1479–91.

Behrenfeld, M. & Kolber, Z. 1999. Widespread iron limitation of phytoplankton in the South Pacific Ocean. *Science* 283:840–3.

Behrenfeld, M. & Milligan, A. 2013. Photophysiological expressions of iron stress in phytoplankton. *Annu. Rev. Mar. Sci.* 5:217–46.

Behrenfeld, M., Boss, E., Siegel, D. & Shea, D. 2005. Carbon-based productivity and phytoplankton physiology from space. *Global Biogeochem. Cy.* 19:GB1006.

Behrenfeld, M., Halsey, K. & Milligan, A. 2008. Evolved physiological responses of phytoplankton to their integrated growth environment. *Philo. Trans. B. Bio. Sci.* 363:2687–2703.

Behrenfeld, M., O'Malley, R., Boss, E., Westberry, T., Graff, J., Halsey, K., Milligan, A., Siegel, D. & Brown, M. 2015. Revaluating ocean warming impacts on global phytoplankton. *Nat. Clim. Change.* 6:323–30.

Behrenfeld, M., Prasil, O., Babin, M. & Bruyant, F. 2004. In search of a physiological basis for covariations in light-limited and light-saturated photosynthesis. *J. Phycol.* 40:4–25.

Bollivar, D. 2006. Recent advances in chlorophyll biosynthesis. *Photosyn. Res.* 90:173–94.

Brown, M., Penta, W., Jones, B. & Behrenfeld, M. 2019. The ratio of single-turnover to multiple-turnover fluorescence varies predictably with growth rate and cellular chlorophyll in the green alga *Dunaliella tertiolecta*. *Photosyn. Res.* 140:65–76.

Chen, Y., Durnford, D., Koblizek, M. & Falkowski, P. 2004. Plastid regulation of *Lhcb1* transcription in the Chlorophyte alga *Dunaliella tertiolecta*. *Plant Physiol.* 136:3737–50.

D'asaro, E. A. 2003. Performance of autonomous Lagrangian floats. *J. Atmos. Ocean. Technol.* 20:896–911.

Denman, K. & Gargett, A. 1983. Time and space scales of vertical mixing and advection of phytoplankton in the upper ocean. *Limnol. Oceanogr.* 28:801–15.

Escoubas, J., Lomas, M., LaRoche, J. & Falkowski, P. 1995. Light intensity regulation of *cab* gene transcription is signaled by the redox state of the plastoquinone pool. *Proc. Natl. Acad. Sci. USA* 92:10237–41.

Falkowski, P. & LaRoche, J. 1991. Acclimation to spectral irradiance in algae. *J. Phycol.* 27:8–14.

Falkowski, P. & Owens, T. 1980. Light-shade adaptation. Two strategies in marine phytoplankton. *Plant Physiol.* 66:592–5.

Fietz, S. & Nicklisch, A. 2002. Acclimation of the diatom *Stephanodiscus neoastraea* and the cyanobacterium *Planktothrix agardii* to simulated natural light fluctuations. *Photosyn. Res.* 72: 95–106.

Fisher, N. & Halsey, K. 2016. Mechanisms that increase the growth efficiency of diatoms in low light. *Photosyn. Res.* 129:183–97.

Frigerio, S., Campoli, C., Zorzan, S., Fantoni, L., Crosatti, C., Drepper, F., Heahnel, W., Cattivelli, L., Morosinotto, T. & Bassi, R. 2007. Photosynthetic antenna size in higher plants is controlled by the plastoquinone redox state at the post-transcriptional rather than transcriptional level. *J. Biol. Chem.* 282:P29457–69.

Fong, A. & Archibald, J. 2008. Evolutionary dynamics of light-independent protochlorophyllide oxidoreductase genes in the secondary plastids of cryptophyte algae. *Eukaryot. Cell* 7: 550–3.

Halsey, K., Milligan, A. & Behrenfeld, M. 2010. Physiological optimization underlies growth rate-independent chlorophyll-specific gross and net primary production. *Photosyn. Res.* 103:125–37.

Halsey, K., O'Malley, R., Graff, J., Milligan, A. & Behrenfeld, M. 2013. A common partitioning strategy for photosynthetic products in evolutionarily distinct phytoplankton species. *New Phytol.* 198:1030–8.

Halsey, H., Milligan, A. & Behrenfeld, M. 2014. Contrasting strategies of photosynthetic energy utilization drive lifestyle strategies in ecologically important picoeukaryotes. *Metabolites* 4:260–80.

Havelkova, H., Prasil, O. & Behrenfeld, M. 2004. Photoacclimation of *Dunaliella tertiolecta* (Chlorophyceae) under fluctuating irradiance. *Photosynthetica* 42:273–81.

Hunsperger, H., Randhawa, T. & Cattolico, R. 2015. Extensive horizontal gene transfer, duplication, and loss of chlorophyll synthesis genes in algae. *BMC Evol. Biol.* 15:16.

Ibelings, B., Kroon, B. & Mur, L. 1994. Acclimation of photosystem II in a cyanobacterium and a eukaryotic green alga to high and fluctuating photosynthetic photon flux densities, simulating light regimes induced by mixing in lakes. *New Phytol.* 128:407–24.

Jans, F., Mignolet, E., Houyoux, P. A., Cardol, P., Ghysels, B., Cuine, S., Cournac, L., Peltier, G., Remacle, C. & Franck, F. 2008. A type II NAD(P)H dehydrogenase mediates light-independent plastoquinol reduction in the chloroplast of *Chlamydomonas. Proc. Natl. Acad. Sci. USA* 105:20546–551.

Jassby, A., & Platt, T. 1976. Mathematical formulation of the relationship between photosynthesis and light for phytoplankton. *Limnol. Oceanogr.* 21:540–7.

Kauss, D., Bischof, S., Steiner, S., Apel, K. & Meskauskiene, R. 2012. FLU, a negative feedback regulator of tetrapyrrole biosynthesis, is physically linked to the final steps of the Mg++-branch of this pathway. *FEBS Lett.* 586:211–6.

Kolber, Z., Prasil, O. & Falkowski, P. 1998. Measurements of variable chlorophyll fluorescence using fast repetition rate techniques: defining methodology and experimental protocols. *Biochim. Biophy. Acta.* 1367:88–106.

Lee, Z., Carder, K., Marra, J., Steward, R. & Perry, M. 1996. Estimating primary productivity at depth from remote sensing. *Appl. Opt.* 35:463–74.

Lepetit, B., Strum, S., Rogato, A., Gruber, A., Sachse, M., Falciatore, A., Kroth, P. & Lavaud, J. 2013. High light acclimation in the secondary plastids containing diatom *Phaeodactylum tricornutum* is triggered by the redox state of the plastoquinone pool. *Plant Physiol.* 161:853–65.

Lewis, M. R. & Smith, J. C. 1983. A small volume, short incubation time method for measurement of photosynthesis as a function of incident irradiance. *Mar. Ecol. Prog. Ser.* 13: 99–102.

Li, Z., Wakao, S., Fischer, B. & Niyogi, K. 2009. Sensing and responding to excess light. *Annu. Rev. Plant Biol.* 60:239–60.

MacIntyre, H., Kana, T., Anning, T. & Geider, R. 2002. Photoacclimation of photosynthesis irradiance response curves and photosynthetic pigments in microalgae and cyanobacteria. *J. Phycol.* 38:17–38.

Milligan, A., Aparicio, U. & Behrenfeld, M. 2012. Fluorescence and nonphotochemical quenching responses to simulated vertical mixing in the marine diatom *Thalassiosira weissflogii. Mar. Ecol. Prog. Ser.* 448:67–78.

Mills, M., Kropuenske, L., van Dijken, G., Alderkamp, A., Berg, G., Robinson, D., Welshmeyer, N. & Arrigo, K. 2010. Photophysiology in two southern ocean phytoplankton taxa: photosynthesis of *Phaeocystis antarctica* (Prymnesiophyceae) and *Fragilariopsis cylindrus* (Bacillariophyceae) under simulated mixed-layer irradiance. *J. Phycol.* 46:1114–27.

Moller, I. & Sweetlove, L. 2010. ROS signalling – specificity is required. *Trends Plant Sci.* 15:370–4.

Mullineaux, C. 2014. Co-existence of photosynthetic and respiratory activities in cyanobacterial thylakoid membranes. *Biochim. Biophys. Acta.* 1837:503–11.

Peltier, G. & Cournac, L. 2002. *Chlororespiration. Ann. Rev. Plant. Biol.* 53:523–550.

Pfannschmidt, T., Nilsson, A. & Allen, J. 1999. Photosynthetic control of chloroplast gene expression. *Nature* 397:625–8.

Pfannschmidt, T., Schutze, K., Brost, M. & Oelmuller, R. 2001. A novel mechanism of nuclear photosynthesis gene regulation by redox signals from the chloroplast during photosystem stoichiometry adjustment. *J. Biol. Chem.* 276:36125–30.

Pfannschmidt, T. & Yang, C. 2012. The hidden function of photosynthesis: a sensing system for environmental conditions that regulates plant acclimation responses. *Protoplasma* 249:S125–36.

Prasil, O., Kolber, Z. & Falkowski, P. 2018. Control of the maximal chlorophyll fluorescence yield by the Qb binding site. *Photosynthetica.* 56:150–62.

Reinbothe, C., Bakkouri, M., Buhr, R., Muraki, N., Nomata, J., Kurisu, G., Fujita, Y. & Reinbothe, S. 2010. Chlorophyll biosynthesis: spotlight on protochlorophyllide reduction. *Trends Plant Sci.* 15:614–24.

Richter, A., Peter, E., Lorenzen, S., Grimm, B. & Czarnecki, O. 2010. Rapid dark repression of 5-aminolevulinic acid synthesis in green barley leaves. *Plant Cell Physiol.* 51:670–81.

Ritchie, R. 2006. Consistent sets of spectrophotometric chlorophyll equations for acetone, methanol and ethanol solvents. *Photosyn Res.* 89:27–41.

Rochaix, J. 2011. Regulation of photosynthetic electron transport. *Biochim. Biophys. Acta.* 1870:375–83.

Shatwell, T., Nicklisch, A. & Kohler, J. 2012. Temperature and photoperiod effects on phytoplankton growing under simulated mixed layer light fluctuations. *Limnol. Oceanogr.* 57:541–53.

Siegel, D., Behrenfeld, M., Maritorena, S., McClain, C. R., Antione, D., Bailey, S. W., Bontempi, P. S. et al. 2013. Regional to global assessments of phytoplankton dynamics from the Sea WiFS mission. *Remote Sens. Environ.* 135:77–91.

Silsbe, G., Behrenfeld, M., Halsey, K., Milligan, A. & Westberry, T. 2016. The CAFE model: A net production model for global ocean phytoplankton. *Global Biogeochem. Cy.* 30: 1756–77.

Smyth, T., Tilstone, G. & Groom, S. 2005. Integration of radiative transfer into satellite models of ocean primary productivity. *J. Geophys. Res.* 110:C10014.

Strand, A., Asami, T., Alonso, J., Ecker, J. & Chory, J. 2003. Chloroplast to nucleus communication triggered by accumulation of Mg-protoporphyrin IX. *Nature* 421:79–83.

Suggett, D., Lefloch, E., Harris, G., Leonardos, N. & Geider, R. 2007. Different strategies of photoacclimation by two strains of *Emiliana huxleyi* (Haptophyta). *J. Phycol.* 43:1209–22.

Sukenik, A., Bennett, J. & Falkowski, P. 1987. Light-saturated photosynthesis – limitation by electron transport or carbon fixation. *Biochim. Biophys. Acta.* 891:205–15.

Tang, E. & Vincent, W. 2000. Effects of daylength and temperature on the growth and photosynthesis of an Arctic cyanobacterium, *Schizothriz calcicole* (Oscillatoriaceae). *Eur. J. Phycol.* 35:263–72.

Toth, S., Schansker, G. & Strasser, R. 2007. A non-invasive assay of the plastoquinone redox state based on the OJIP-transient. *Photosyn. Res.* 93:190–203.

Westberry, T., Behrenfeld, M., Siegel, M., Anning, T. & Geider, R. 2008. Carbon-based primary productivity modeling with vertically resolved photoacclimation. *Global Biogeochem. Cy.* 22:GB2024.

Vandenhecke, J., Bastedo, J., Cockshutt, A., Campbell, D. & Huot, Y. 2015. Changes in the Rubisco to photosystem ratio dominates photoacclimation across phytoplankton taxa. *Photosyn. Res.* 124:275–91.

Van de Poll, W., Visser, R. & Buma, A. 2007. Acclimation to a dynamic irradiance regime changes excessive irradiance sensitivity of *Emiliania huxleyi* and *Thalassiosira weisflogii*. *Limnol. Oceanogr.* 52:1430–38.

Verity, P. 1981. Effects of temperature, irradiance and daylength on the marine diatom *Leptocylindrus danicus* Cleve. Photosynthesis and cellular composition. *J. Exp. Mar. Biol. Ecol.* 55: 79–91.

Supporting Information

Additional Supporting Information may be found in the online version of this article at the publisher's web site:

Figure S1. Example of chlorophyll fluorescence transient measured using fast repetition rate fluorometry (FRRf).